ANGULAR DISTRIBUTION

PHYSICS DEGREE Academic Year 2021-2022

Group 17, cohort 3
Rachele Cicioni
Maria Sharon Di Spena
Giacomo Guastella

January 3, 2022

Abstract

The aim of the experiment is the study of a ^{60}Co radioactive source with unknown activity through the measuring of two Nai(Tl) detectors efficiency and the correlation in the angular distribution of gamma radiation emitted by the source.

1 Experimental SET-UP

The experimental apparatus is composed by a ^{60}Co source and a ^{241}Am, two NaI(Tl) scintillation detectors: both can vary the distance from the source, only one can also rotate around it. The two detectors operate at HV = 700 V and HV = 1200 V via the CAEN N472 module. The Set-Up is also composed of a A crate NIM composed by a Philips 744 Quad Linear Gate FAN-IN-FAN-OUT and Constant Fraction Time Discriminators (CFTDs), a Coincidence Logic Unit module and a CAEN DT5720 digitizer.

2 Calibration and optimization of the detectors

In order to have a greater reliability of the acquired data, it is necessary a preliminary preparation of the detectors and a study of the effects of the electronic apparatus on the signal recorded by them. Afterward, the energy calibration of the detectors is performed, using the known energies of the photons emitted by the ^{60}Co source, at 1173 keV and at 1333 keV, and an additional radioactive source, ^{241}Am, that emits photons at 59 keV, in order to improve the accuracy of the calibration.

Preparation of the detectors

With the ^{60}Co inserted in the collimator, the preamplification signals coming directly from the FAN-IN-FAN-OUT module are analyzed and are compared with the signals coming from the CFTD. For the first of these, polarity, amplitude, rising and falling time are recorded, and the amplitude corresponding to the peaks of the 1333 keV transition is identified. All these values are reported in the **Table 1**, for both the scintillators. The error is taken considering the sensitivity of both cursors of the oscilloscope.

Detector	Fall time (ns)	Rise time (ns)	$V_{max_{1333keV}}(mV)$
1	80 ± 20	670 ± 20	-160 ± 8
2	70 ± 20	690 ± 20	-160 ± 8

Table 1: Characteristic parameters of the signals from the detectors directly connected from the FAN-IN-FAN-OUT module to the oscilloscope.

The second output of the FAN-IN-FAN-OUT is therefore sent to the CFTD, and the output prompt signal is observed on the oscilloscope, varying the width and the delay set on the CFTD. Such variations are measured on the oscilloscope, and it is noted that the values setted are not exactly the ones observed, probably because of the alterations due to the electronic apparatus. For this reason, from this point on, the characteristic values of the signal are measured directly on the oscilloscope.

In order to reduce the effects of electronic equipment noise, it is necessary to set the threshold value for the CFTD. This is done by connecting the anode signal from the FAN-IN-FAN-OUT and one of the outputs of the CFTD to the oscilloscope. Observing the variation of the anode signal with the variation of the threshold set on the CFTD, the latter is fixed to the minimum value needed to cut the noise. The values of threshold for both the detectors are reported in the **Table 2**.

Detector	CFTD threshold
1	$48 \pm 4mV$
2	$36 \pm 4mV$

Table 2: Values of CFTD threshold for both the detectors.

Analysis for different statistics

At this point it is possible to proceed with the acquisition of the ^{60}Co spectrum, and then with the calibration in energy of the detectors. Before doing that, it is interesting to study the behavior of the photopeak centroid error with the varying of the number of acquired events, in order to obtain the maximum precision in the energy calibration, i.e. in the energy of the photons measured in the following sessions. To do this, the anode signal from the FAN-IN-FAN-OUT is connected to the input of the digitizer, while the delayed output is connected to the input of the Coincidence Unit. Selecting the OR logical signal output, this one in used as the trigger for the digitizer. Then a series of Cobalt and Americium spectra are acquired for different time intervals using the VERDI software, at the minimum time step available, $10s$, $30s$, $45s$ and $60s$, noting that different time intervals corresponds to different number of acquired events, and so to different statistics in the gamma spectrum. The Americium source is used in order to improve the accuracy of the following energy calibration. The procedure is repeated for both the detectors. From the acquired spectra, it is possible to fit the peaks with a Gaussian and to determinate the centroid value and its error. The obtained result are reported in the **Table 3** and **Table 4**, for both the detectors.

Acquisition time (s)	Entries	$\mu[ch]$	$\sigma[ch]$	FWHM $[ch]$	Resolution %
6	53000 ± 200	6736 ± 2	155 ± 2	365 ± 4	5.42 ± 0.06
10	130000 ± 400	6735 ± 1	154 ± 1	363 ± 3	5.39 ± 0.04
30	385000 ± 600	6735 ± 1	158 ± 1	371 ± 1	5.51 ± 0.02
45	580200 ± 800	6735 ± 1	158 ± 1	373 ± 1	5.54 ± 0.02
60	773000 ± 900	6772 ± 1	154 ± 1	364 ± 1	5.37 ± 0.02

Table 3: Gaussian fit values for the peak at 1333 keV for **Detector 1**.

Acquisition time (s)	Entries	$\mu[ch]$	$\sigma[ch]$	FWHM $[ch]$	Resolution %
3	18900 ± 100	6244 ± 3	151 ± 3	354 ± 6	5.68 ± 0.09
10	117100 ± 300	6242 ± 1	153 ± 1	361 ± 3	5.78 ± 0.04
30	381200 ± 600	6244 ± 1	149 ± 1	352 ± 2	5.64 ± 0.03
45	378700 ± 600	6243 ± 1	152 ± 1	357 ± 2	5.71 ± 0.02
60	731500 ± 900	6241 ± 1	149 ± 1	351 ± 1	5.62 ± 0.02

Table 4: Gaussian fit values for the peak at 1333 keV for **Detector 2**.

As was expected, for both the detectors the centroid error decreases with the increasing of the number of acquired events, while the better resolution is obtained for the spectra with the greater number of entries. Note that for the Detector 2 the number of entries in $45s$ seems to be lower than the number of entries in $30s$. This is probably due to the fact that the Detector 2 is placed at a bigger

distance from the sources, so it is possible that a certain number of events is lost during the acquisition of the spectra. Also note that the peak at 1333 keV is at a lower channel respect to the one expected (10000). This is due to the fact that the voltage applied to the scintillator dynodes is probably lower than it should be.

Energy calibration

In order to calibrate in energy the detectors, a three point linear fit is performed, using the information about the energy of the emitted photons from the ^{60}Co sources (1173 keV and 1333 keV) and from the Americium source (59 keV). Having studied the variation of the error on the mean and of the resolution of the spectra with the variation of the number of events acquired, the spectra with the highest resolution and the least error are selected, i.e. the ones taken in $60s$ and with the greater number of events, in order to have a better calibration accuracy, for both the detectors. The values used for the calibration are collected in the following **Tables 5** and **Table 6**.

Energy (keV)	Peak centroid $[ch]$	Peak width (FWHM) $[ch]$	Resolution %
59	321.6 ± 0.6	289 ± 1	89.9 ± 0.5
1773	5957.1 ± 0.5	376 ± 1	6.31 ± 0.02
1333	6772.1 ± 0.5	364 ± 1	5.37 ± 0.02

Table 5: Values for the energy calibration of the **Detector 1**.

Energy (keV)	Peak centroid $[ch]$	Peak width (FWHM) $[ch]$	Resolution %
59	337.4 ± 0.4	131 ± 1	38.8 ± 0.2
1773	5056.2 ± 0.5	369 ± 1	7.30 ± 0.02
1333	6241.1 ± 0.5	351 ± 1	5.62 ± 0.02

Table 6: Values for the energy calibration of the **Detector 2**.

The linear fit is performed using the relation $E_{keV} = \beta + \alpha E_{Ch}$. Note that the high value of resolution for the Americium peak is due to the fact that the ideal operating range of the NaI(Tl) scintillators is on energies of the order of MeV. The linear fits for both the detector are shown in the following **Figure 1**, together with the fit parameters and with an example of the calibrated spectra.

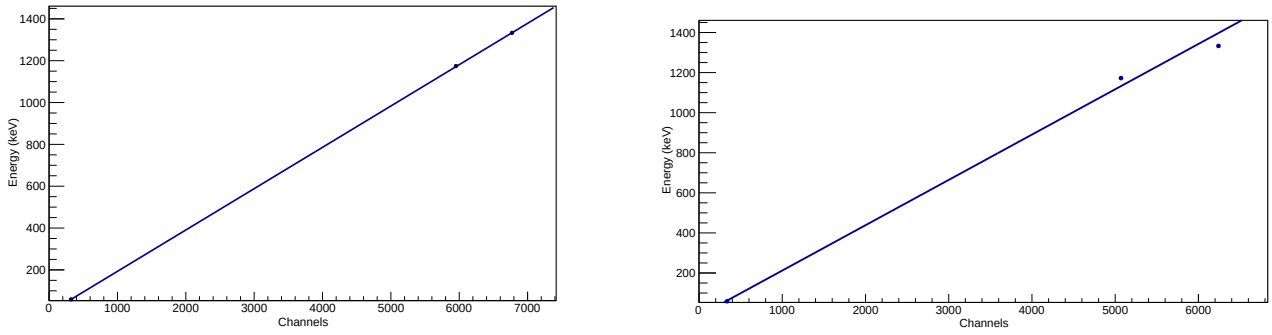

Figure 1: Linear fit for the calibration in energy of the **Detector 1** and **Detector 2**.

	$\beta(keV)$	$\alpha(keV/ch)$
Det 1	-4.4 ± 0.1	0.1976 ± 0.0001
Det 2	-13.91 ± 0.09	0.2261 ± 0.0001

Table 7: Values for the energy calibration of the **Detector 1** and **Detector s**.

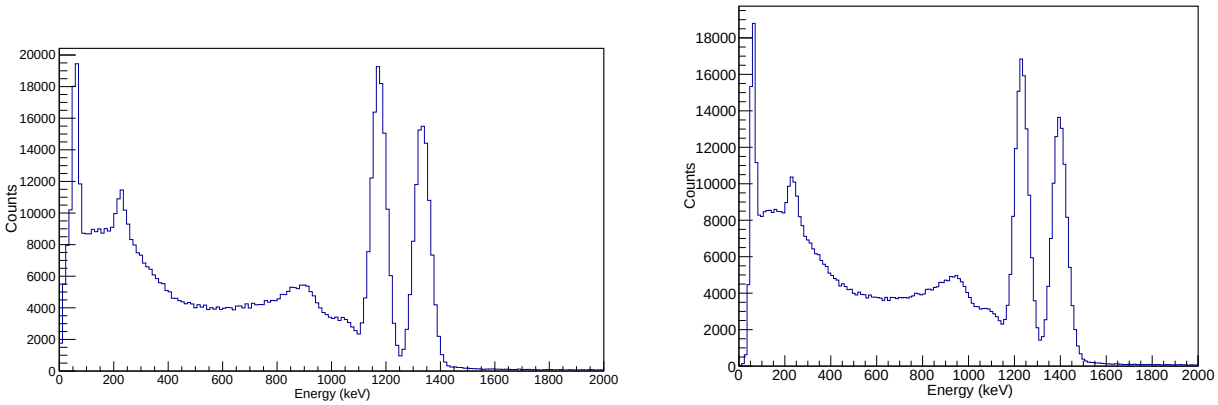

Figure 2: Energy spectrum from the **Detector 1** and **2** with ^{60}Co and ^{241}Am sources.

Optimization of the resolution

A further improvement of the acquired spectra can be obtained optimizing the duration of the integration window used by the data acquisition software VERDI, the LONG GATE, from which depends the resolution of the spectra. In order to do this, the Detector 1 is placed at a distance $d_1 = 12$ cm from the source, while the Detector 2 is placed at $d_2 = 22$ cm. Values of the long gate from 200 to 600 are tested taking different data acquisitions. The better results of resolution, equal to $5,41\%$ for the Detector 1 and $5,58\%$ for the Detector 2, are obtained for a long gate value of 300 for both the detectors. This value is therefore fixed for all the subsequent acquisitions.

3 Realization of coincidences

The two square signals output from the CFTD related to the two detectors are connected to the oscilloscope and, using the appropriate cursors, their width is measured. The signal widths are respectively (100 ± 20)ns for Detector 1 and (100 ± 20)ns for Detector 2. By connecting both signals to the oscilloscope it is observed that they overlap without the need to delay any of the signals. The AND of the two square signals is realized through the CFTD and the output is sent to the trigger of the digitizer.

4 Geometric corrections

Considering the configuration of the previous session, we have the two detectors with an angle of 180° between them. The number of counts expected for each detector is given by:

$$N_i = A\varepsilon_i^{int}\frac{\Omega_i}{4\pi} = A\varepsilon_i^{abs} \tag{1}$$

where ε_i^{int} and ε_i^{abs} are the intrinsic and absolute efficiency of the detectors reported in **Table 10** of the next section, A is the ^{60}Co activity equal to 422 kBq[1] and Ω_i is the solid angle subtended by the detector. The expected number of counts considering the coincidences, i.e. putting the two detectors in logic unit AND, is given by:

$$N = A\varepsilon_1^{int}\varepsilon_2^{int}\frac{\Omega_1}{4\pi}\frac{\Omega_2}{4\pi} = A\varepsilon_1^{abs}\varepsilon_2^{abs}$$

This number of counts consider an isotropic distribution of gamma rays. Therefore it must be multiplied by an anisotropy factor given by:

$$a = \frac{A(180°) - A(90°)}{A(90°)} \simeq 17\%$$

where A(θ) is given by **Eq.2**. The **Table 8** shows the theoretical value of counts N per second and the measured value acquired through the VERDI program. The two values of N are in agreement within

[1]This value was taken from the data tabulated by the didactic center considering the sample 156 of ^{60}Co.

$N_{expected}(Hz)$	$N_{measured}(Hz)$
$(6.96\pm0.06)\cdot10^1$	$(6.8\pm0.8)\cdot10^1$

Table 8: Theoretical expected value and measured value of the counts per second in logic unit AND.

the error limits. This result also assures us the validity of the experimental efficiency value.
To estimate the systematic error due to a displacement of the source with respect to the rotation axis, we put the two detectors in logical unit OR and we take measurements of 5 minutes at different values of θ angles: 0°, 20°, 40°, 50°, 70°, 90°. Since we are in logic unit OR we expect isotropy in the counts, i.e. a constant value as the angle varies. The values obtained are shown in the **Table 9)**. As can be seen, the counts are not constant. In particular we see a large discrepancy at 0°and 40°. To investigate further the reason for this discrepancy the timestamp for each acquisition is seen. At these two angles, the acquisition was not uniform. We then tried to normalize with respect to the timestamp and we obtained the results of **Table 9**. As can be seen from the results it's not possible to normalize precisely with respect to the acquisition times because a precise estimate of the normalization time is not available. For this reason it was decided to neglect these two values for the subsequent analysis and take the non-normalized values. By observing the **Figure 3**, geometric considerations can be made. From the **Eq. 1** we have that:

$$N \propto \Omega = \frac{\pi r^2}{d^2}$$

where d is the distance between the rotation axis and the detector and r the detector beam. Considering a displacement of the source from the axis of rotation by a length L, we have that:

$$N \propto \Omega = \frac{\pi r^2}{d'^2}$$

where d' is the new source-detector distance. From geometric considerations:

$$d - d' \simeq L\cos\alpha = L\sin\theta$$

$$d' = d - L\sin\theta$$

And so:

$$\Omega \propto \frac{1}{d'^2} = \frac{1}{(d - L\sin\theta)^2}$$

A further corrective term can be considered due to the effective area of the detector $A' = A\cos\gamma$:

$$N \propto \Omega \propto \frac{1}{(d - L\sin\theta)^2}\cos\gamma = \frac{1}{(d - L\sin\theta)^2}\frac{D}{d'} \propto \frac{1}{(d - L\sin\theta)^3}$$

The graph in the **Figure 3** shows the experimental data with a fit of a function of the type:

$$f(\theta) = K\frac{1}{(d - L\sin\theta)^3}$$

Considering $d = (22.0 \pm 0.5)cm$ the values of L and K obtained from the fit are:

$$L = (1.7 \pm 0.7)\cdot10^{-2}cm$$

$$K = (4.185 \pm 0.003)\cdot10^5 cm^{-3}$$

where L is the displacement of the source from the rotation axis.

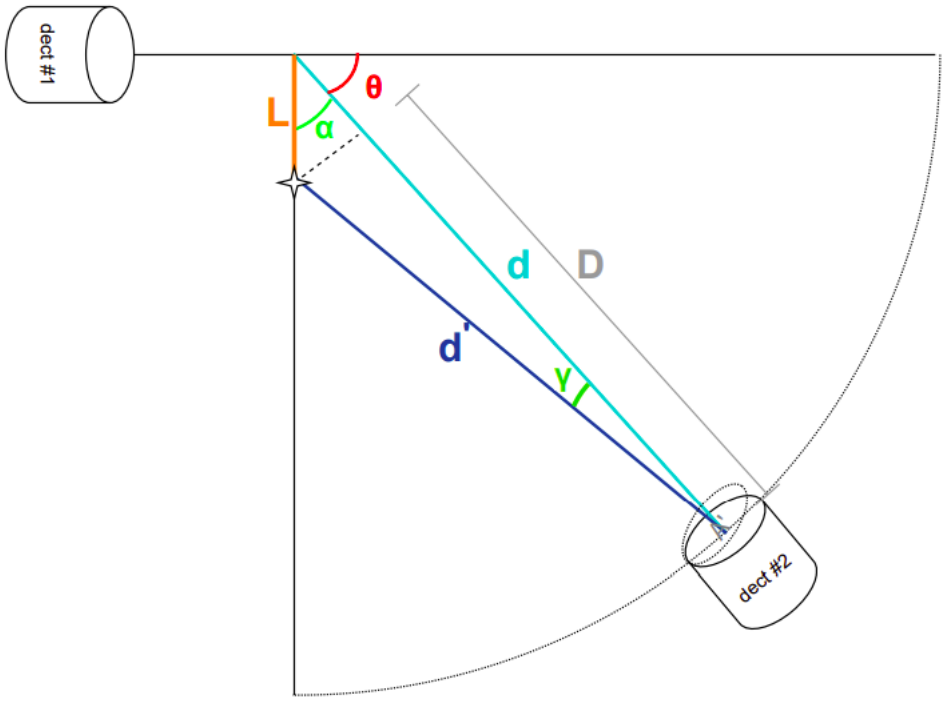

Figure 3: Scheme of the experimental set-up.

$\theta(^\circ)$	Counts	Normalized counts
0	337700±600	56200±200
20	3932000±2000	52400±200
40	3581000±2000	52700±200
50	3940000±2000	52529±200
70	3939000±2000	52500±200
90	3938000±2000	

Table 9: Counts of detector 2 in logical unit AND at different values of θ.

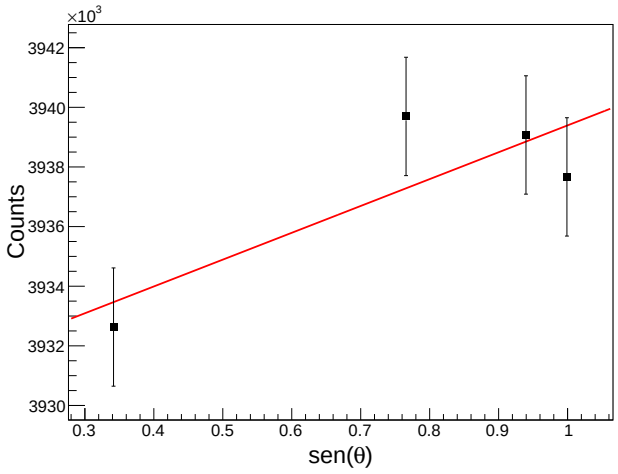

Figure 4: Counts of detector 2 in logical unit AND as a function of $\sin\theta$.

5 Efficiency Measurements

In order to estimate the detectors efficiency, two different techniques are used: the first measurement of the efficiency is carried out using the two photons method, the second one with the sum peak method. The two methods are applied to the same data set acquired in logic unit "OR", with the movable detector at 180° with respect to the other, with Detector 1 at 12 cm from the source, and the other at 22 cm.

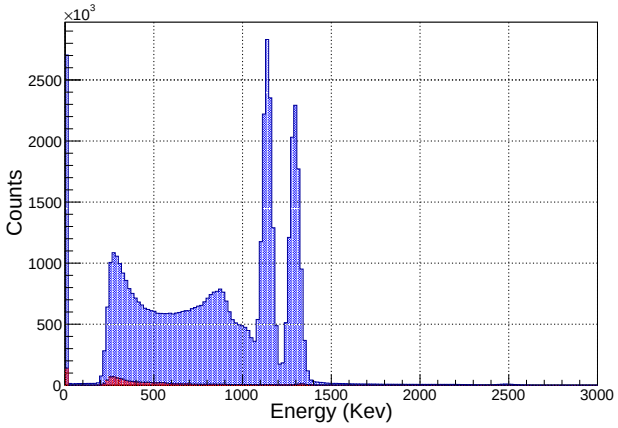

Figure 5: Calibrated in energy spectrum of Detector1: in blue the not corrected spectrum, in red the properly scaled background.

It is acquired ten datasets of 10 minutes each and the analysis is applied to all ten sample and to the sum of these in order to see possible differences at higher statistics. In order to avoid a systematic error bound to the counts in determined regions, it's fundamental to subtract a properly scaled background. To obtain such background, a measurement is made during the night between the laboratory sessions of a 20 hours acquisition without any radioactive sources. It's important to consider that to have consistency, the background must be time scaled with the dataset of the efficiency measurements. Because the count rate is different between the source run and the background run, it is important to take into account the dead time of the acquisition system. In the background sample, the dead time is safely assumed to be null. To estimate the dead time in the source run, the CAEN scaler is used since, not having to analyze the data, it returns the correct count rate. So a 3 minutes measurement is acquired with both the digitizer and the CAEN scaler, and the number of entries of the trigger of the digitizer. It is possible to estimate the factor:

$$Q_{DT} = \frac{\#_{Digitizer}}{\#_{Scaler}} = \frac{2332257}{2390186} = (97.6 \pm 0.1)\%$$

where the errors of the counting are given by a Poissonian distribution ($\sqrt{N}$), and the error of the factor is obtained by propagation. Therefore, it is possible to take into account the different in count rate, the 97 % of the normalized background is subtracted, as can be seen in **Figure 5**.

5.1 Two Photons Method

The coincidence method exploit the coincidence between two detectors: in all events where Detector 1 sees an energy deposit of 1173 keV a 1333 keV range is also emitted in coincidence. The fraction of events where this gamma is detected by Detector 2 gives us an estimate of the efficiency of the detector itself. First of all is important to define this quantities: N_{ij} is the number of events collected by detector j, in correspondence of the peak i. For example: N_{12} is the number of events where Detector 1 revealed a photon of energy 1173 keV and Detector 2 revealed in coincidence a 1333 keV photon. In order to be consistence, it is important to specify that to extrapolate the number of counts under a peak, it is compute the integral of the bins in the same region of 160 keV for all the datasets and all the peaks. This allows to avoid any discrepancy in the counting.
Therefore, it is possible to compute the absolute efficiency of the detectors $\varepsilon_i^{abs} = \frac{N_{ji}}{N_i}$, where N_i is the number of events acquired under the 1173 keV peak of detector j. The results can be seen in **Table 10**.

Set	N_{12}	N_{21}	N_1	N_2	ε_1^{abs}	ε_2^{abs}
1	2500 ± 50	2460 ± 50	459400 ± 700	1165000 ± 1000	0.0053 ± 0.0001	0.0021 ± 0.0001
2	2520 ± 50	2470 ± 50	483300 ± 700	1226000 ± 1000	0.0051 ± 0.0001	0.0021 ± 0.0001
3	2360 ± 50	2380 ± 50	455100 ± 700	1144000 ± 1000	0.0052 ± 0.0001	0.0021 ± 0.0001
4	2450 ± 50	2530 ± 50	477700 ± 700	1200000 ± 1000	0.0053 ± 0.0001	0.0020 ± 0.0001
5	2520 ± 50	2480 ± 50	473200 ± 700	1194000 ± 1000	0.0052 ± 0.0001	0.0021 ± 0.0001
6	1800 ± 40	1750 ± 40	336200 ± 600	849500 ± 900	0.0052 ± 0.0001	0.0021 ± 0.0001
7	2620 ± 50	2470 ± 50	483100 ± 700	1222000 ± 1000	0.0051 ± 0.0001	0.0021 ± 0.0001
8	2490 ± 50	2500 ± 50	469100 ± 700	1183000 ± 1000	0.0053 ± 0.0001	0.0021 ± 0.0001
9	2500 ± 50	2450 ± 50	490300 ± 700	1235000 ± 1000	0.0050 ± 0.0001	0.0020 ± 0.0001
10	2390 ± 50	2400 ± 50	452800 ± 700	1145000 ± 1000	0.0053 ± 0.0001	0.0021 ± 0.0001
Sum	24200 ± 200	20800 ± 100	4484000 ± 2000	11570000 ± 3000	0.00464 ± 0.00003	0.00209 ± 0.00001

Table 10: Results for the coincidence method and the estimated efficiency for all the datasets (in red the sample with a significant lower counting) and for the sum of these (green) for both the detectors.

As can be seen in the table above, the efficiency remain constant for the whole acquisition, so it is correct to assume that the efficiency would not change during the laboratory session. However, the results obtained for the sum of all the samples is slightly under the value of the single dataset. This is due to the fact that a strange behaviour appears in the large statistics analysis. As can be seen in **Figure 6**, when a photon with energy 1332 keV is collected in the detector 1, sometime a second gamma of energy 1332 keV is collected by the detector 2. This is probably due to some false coincidence that must be taken into account. So the efficiency obtained from the sum of all the samples is estimated subtracting this false coincidences that probably introduces a systematic error that affect the single samples. Fot this reason the efficiency obtained from the sum of all the dataset is the best estimate (in green in the tables). It is possible to compute the number of false coincidences of two uncorrelated photons in a measurement: considering an overlap time for the coincidence of $\Delta t = 100ns$, as seen in **Paragraph 3**: $C_{R_{false}} = \Delta t C_{R_1} \cdot C_{R_2}$ that introduces an error of $\sim 1\%$ in the count rate.

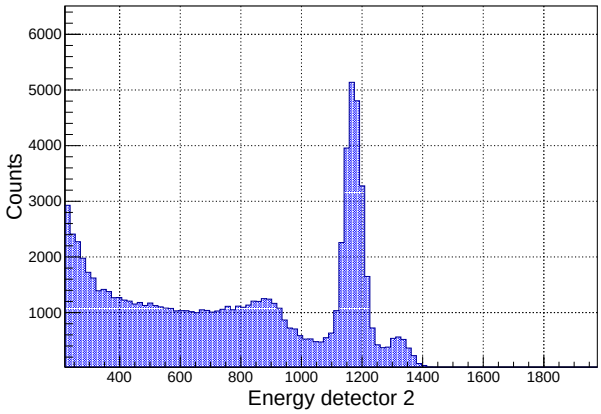

Figure 6: Spectrum of the Detector 2 conditioned by the revealing of a photon of 1333 keV by Detector 1, for the "sum" sample.

It is possible now to compute the intrinsic efficiency of the detectors considering the solid angle Ω_i subtended by the detector i with $r_i = 4cm$ the radius of the detector:

$$\varepsilon_i^{int} = \frac{4\pi}{\Omega_i}\varepsilon_i^{abs} = \frac{4d_i^2}{r^2}\varepsilon_i^{abs}$$

The results for the two detectors are:

$$\varepsilon_1^{int} = 0.167 \pm 0.003 \qquad \varepsilon_2^{int} = 0.253 \pm 0.003$$

5.2 Sum Peak Method

The existence of a peak at 2506 keV allows to provide a measurement of the absolute efficiency of the detector. The probability of detecting both gammas in the same detector is given in a first approximation by the efficacy product to reveal the individual gamma ($\varepsilon_{2506} = \varepsilon_{1173+1333}$). From a comparison of counts in the peaks at 1173, 1333 and 2506 keV, it will be possible to obtain an estimate of the detector efficiency at a given distance from the source. Therefore, since the counts under an energy peak is given by the product of efficiency of the detector at that energy times the source activity the detectors efficiencies can be compute as the ratio of events counted under the peak at 2506 keV and the events under the energy peaks. In this way, it is possible to obtain a value for the efficiency without the value of the activity of the source. Therefore, the absolute efficiency of the detector i can be compute as:

$$\varepsilon_i^{abs} = \frac{N_{2506}^i}{N_{1173}^i + N_{1333}^i}$$

As said before, the properly scaled background is subtract from each set and for the sum of each set in order to have consistent results.

Set	N_{1173}	N_{1333}	N_{2506}	ε_1^{abs}
1	1167000 ± 1000	850400 ± 900	7680 ± 90	0.00381 ± 0.00004
2	1227000 ± 1000	893900 ± 900	8040 ± 90	0.00379 ± 0.00004
3	1145000 ± 1000	838500 ± 900	7530 ± 90	0.00380 ± 0.00004
4	1200000 ± 1000	878900 ± 900	7880 ± 90	0.00379 ± 0.00004
5	1194000 ± 1000	875300 ± 900	7870 ± 90	0.00380 ± 0.00004
6	8500000 ± 900	622300 ± 800	5760 ± 80	0.00392 ± 0.00004
7	1222000 ± 1000	894500 ± 900	8000 ± 90	0.00379 ± 0.00004
8	1183000 ± 1000	866600 ± 900	7770 ± 90	0.00379 ± 0.00004
9	1235000 ± 1000	903000 ± 900	7990 ± 90	0.00374 ± 0.00004
10	1145000 ± 1000	835800 ± 900	7500 ± 90	0.00379 ± 0.00004
Sum	11570000 ± 3000	8460000 ± 3000	76000 ± 300	0.00380 ± 0.00001

Table 11: Results for the sum peak method and the estimated efficiency for all the datasets (in red the sample with a significant lower counting) and for the sum of these (in green) for Detector 1.

Set	N_{1173}	N_{1333}	N_{2506}	ε_2^{abs}
1	461500 ± 700	371800 ± 600	1920 ± 40	0.00299 ± 0.00004
2	485400 ± 700	390300 ± 600	2040 ± 50	0.00232 ± 0.00004
3	455200 ± 700	364500 ± 600	1890 ± 40	0.00230 ± 0.00004
4	477900 ± 700	382300 ± 600	2030 ± 50	0.00236 ± 0.00004
5	473400 ± 700	379900 ± 600	1860 ± 40	0.00217 ± 0.00004
6	336500 ± 600	269800 ± 500	1400 ± 40	0.00230 ± 0.00004
7	483300 ± 700	386900 ± 600	2020 ± 50	0.00232 ± 0.00004
8	469400 ± 700	375500 ± 600	1920 ± 40	0.00228 ± 0.00004
9	490500 ± 700	392400 ± 600	2080 ± 50	0.00235 ± 0.00004
10	453000 ± 700	361700 ± 600	1760 ± 40	0.00216 ± 0.00004
Sum	4584000 ± 2000	3673000 ± 2000	18500 ± 100	0.00224 ± 0.00001

Table 12: Results for the sum peak method and the estimated efficiency for all the datasets (in red the sample with a significant lower counting) and for the sum of these (in green) for detector 2.

As can be seen from the table above, among the error boundaries the efficiency again remain constant. However, the results obtained from the two different method are not compatible with each other. This is probably due to a systematic error that affects the samples similar to the one visible in **Figure 6**. In fact, in the last method the peak around 2506 keV is not well shaped so it is used a larger integration range of 250 keV to consider the whole peak. This is probably due to some false expected false coincidence. It is expected to be seen two peaks nearby the sum peak, that should appear at 2346

keV and 2665 keV, corresponding to events in which two photons of the same energy are detected in the same detector. Since those peaks are not visible in no one of the spectra acquired, it means that the structure of the sum peak is the superposition of the three peaks that arise in a range of 250 keV (**Figure 7**).
Obviously, the same error affects the estimate of the intrinsic efficiency:

$$\varepsilon_1^{int} = 0.137 \pm 0.003 \qquad \varepsilon_2^{int} = 0.271 \pm 0.003$$

For this reason, the sum peak method can not be considered an effective method to compute the efficiency of the detectors. It is not possible to compute quantitatively the entries in the two peaks around the expected one, so it is not possible do subtract the false coincidence from the 2506 keV one. Therefore, the two photons method is the chosen one to be the most precise.

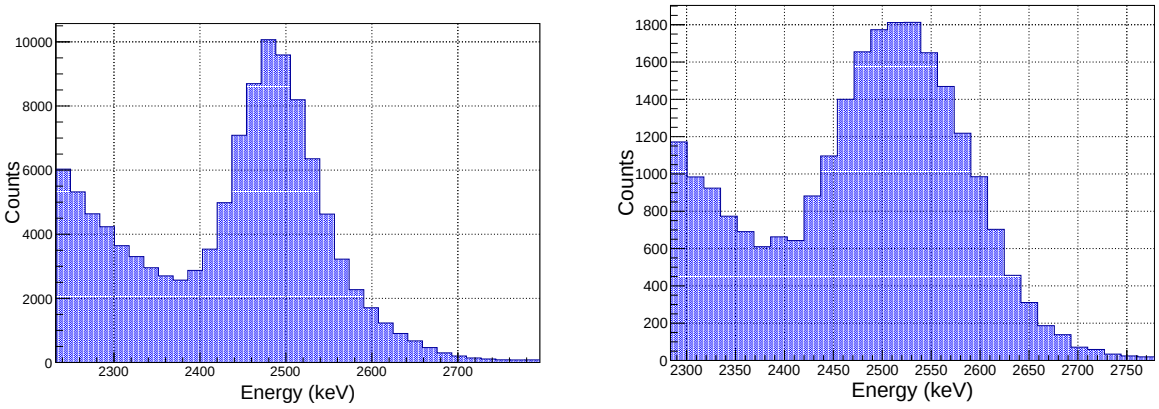

Figure 7: The sum peak expected at 2506 keV for the Detector 1 (first figure) and Detector 2 (second figure), form the "sum" sample

Lastly, the analysis of the ten samples expose a systematic error that affects the acquisition system. As can be seen in red in **Table 10**, **11** and **13** a set registered a lower count respect all the others. To understand the origin of this behaviour, it is studied the timetag of the Digitizer to understand if there is been a failure in the acquisition. As can be seen in **Figure 8**, comparing two different samples (the number 6 and number 9), in the first one there is a gap at the end of the acquisition time of the Digitizer.

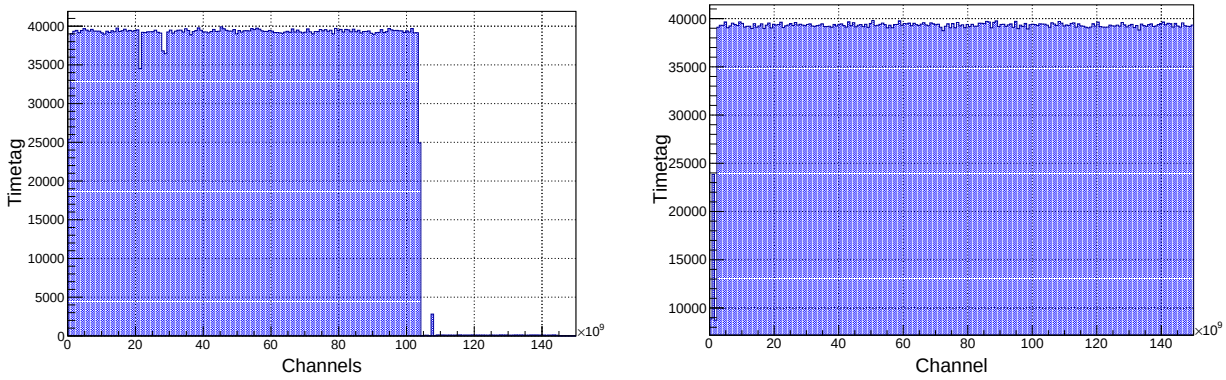

Figure 8: Graphs of the timetag of the Digitizer for the sample 6 in red in the tables (first figure) and the sample 9 (second figure)

Although this error probably does not affect the efficiency measurements as it only entails a rescaling of the quantities, it is important to note as it affects the data in the Geometric corrections section, and the coincidence in the angular distribution's one.
All the results obtained of detector 2 are valid only at the position in which the apparatus is set. Due

to the geometry of the detectors and the source, as described in **Section 4**, the distance of the detector change in respect to the angle with the source due to the misalignment to the source. The correct efficiency at the various angle must be taken into account the dependence of the distance d_2 from the angle θ.

6 Angular Correlation

In order to study the angular correlation between the two gammas emitted by the beta decay of ^{60}Co, six different samples is taken at different angles moving Detector 2(0°, 20°, 40°, 50°, 70°, 90° with respect of the source axis and Detector 1) with the logical condition of AND, since we are interested only in the events in which both the gammas reach the detector. In **Figure 9**, is it possible to see an example of the correlation matrix between the two spectra in AND mode acquisition at 0°. There are the two main peaks: the first is realized when the emitted gammas of 1173 keV is revealed by the Detector 1 and Detector two reveal the one of 1333 keV, the second one is realized when the Detector 2 reveal the 1173 photon and the other reveal the 1333 one. The other two small peaks around 850 keV and 1050 keV could be events in which a single photon is Compton back-scattered in detector 1 releasing there most of its energy and then absorbed in Detector 2 with its remaining energy.

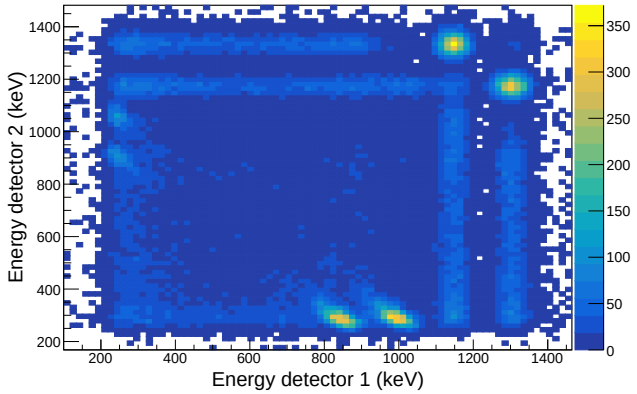

Figure 9: Correlation matrix between coincidence at 0° in AND mode acquisition.

For the purpose of the analysis, it's important to discuss both the scenarios: **1**: when a γ_{1173} hits the Detector 1 and γ_{1333} hits Detector 2, and **2**: when a γ_{1333} hits the Detector 1 and γ_{1173} hits Detector 2. An eventual difference between the two results could expose a systematic error in the apparatus. The expected normalized angular distribution follows the trend:

$$A(\theta) = \frac{C(\theta)}{C(90°)} = 1 + acos^2(\theta) + bcos^4(\theta) \tag{2}$$

where $a = \frac{1}{8}$ and $b = \frac{1}{24}$. In order to obtain consistence measurements, again the proper scaled background is subtract from the samples. The events are acquired in both the cases described above with a poissonian error associated. Every sample is obtained from the same time acquisition of 30 minutes. In **Table 13**, N_i and A_i refers to the cases described above.

Angle (°)	N_1	N_2	A_1	A_2	A_{th}
0	6520 ± 80	6140 ± 80	1.15 ± 0.02	1.13 ± 0.02	1.17
20	6430 ± 80	5920 ± 80	1.13 ± 0.02	1.09 ± 0.02	1.14
40	6100 ± 80	5890 ± 80	1.08 ± 0.02	1.08 ± 0.02	1.09
50	6000 ± 80	5880 ± 80	1.05 ± 0.02	1.08 ± 0.02	1.06
70	5700 ± 80	5560 ± 80	1.01 ± 0.02	1.02 ± 0.02	1.02
90	5670 ± 80	5450 ± 80	1.00 ± 0.02	1.00 ± 0.02	1.00

Table 13: Results for the angular correlation study of the ^{60}Co beta decay.

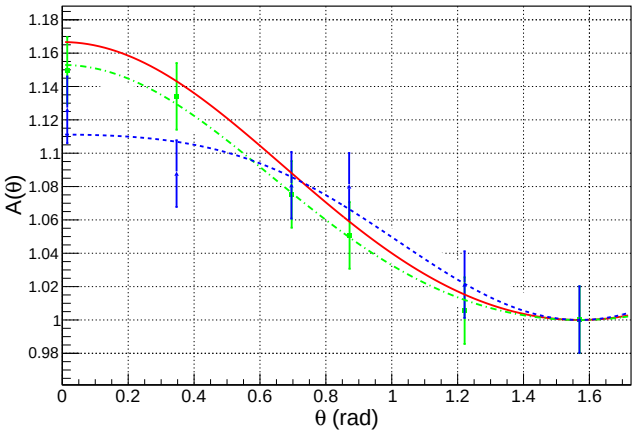

Figure 10: Comparison of the angular distribution trend: in green A_1, in blu A_2, in red the theoretical expectation.

	a	b	χ^2 / ndf
A_1	0.09 ± 0.05	0.06 ± 0.07	$0.2/4$
A_2	0.19 ± 0.08	-0.08 ± 0.07	$2/4$

Table 14: Fit parameters of the angular distribution trend. The colors of the rows take up the colors of the interpolation curves.

As can be seen in **Figure 10** and **Table 14**, the two cases presents a different behaviour, notwithstanding that both follows the expected trend. The first (in green) is the best estimation of the fitting parameters. As a matter of fact, every value among the error boundaries, is compatible with the expected curve. The second curve, in blue, still follows the expected trend but, at low angles, moves away from the theoretical (red) line. Also in this case, the values of the fit are compatible with a and b of the theory. Despite of all this, the fundamental information resides in the χ^2. The values obtain are too low which informs that there is an overestimation of the errors. The too large values of them are the reason why the fitting values are compatible with the expected curve, but, as can be seen in the Figure above, they do not follow very well the theory. There seems to be an attenuate factor that affects mostly the second case. The difference between the experimental curve and the theoretical one may be attributable to two main factor: the not perfect efficiency of the detectors, amplified by the difference in distance of the two detectors from the source, and the geometry of the system. Because of the misalignment of the movable detector with the rotation axis in respect of the source, the angular distribution is affects by a systematic error highlighted in **Paragraph 4**. Even by multiplying the correction function of θ normalized, the fit does not improve significantly.

Conclusion

In conclusion, it is measured the efficiency of the detectors and the best estimate is given by the coincidence method, because it has been possible to correct some systematic errors. The absolute and intrinsic efficiencies when the detectors lie one in front of the other are: $\varepsilon_1^{abs} = 0.00464 \pm 0.00003$, $\varepsilon_2^{abs} = 0.00209 \pm 0.00001$ and $\varepsilon_1^{int} = 0.167 \pm 0.003$, $\varepsilon_2^{int} = 0.253 \pm 0.003$. Due to a systematic error in the geometry of the apparatus the efficiency of the detector depend on the angle.
It is verified the angular distribution trend within the experimental errors, even if the χ^2 reveal that this result is tainted by an overestimation of the errors in the fit parameters.